AGU100 ADVANCING EARTH AND SPACE SCIENCE

Water Resources Research

RESEARCH ARTICLE
10.1029/2017WR021831

Key Points:
- Despite minimal seasonality in rainfall, runoff generation, or the rainfall-runoff ratio, there is strong seasonality in groundwater recharge
- Extended periods of high catchment wetness, rather than storm events, were the primary driver of groundwater recharge at the Maimai watershed
- Unfractured low permeability bedrock and an efficient preferential flow network explain why runoff generation and recharge were uncorrelated

Supporting Information:
- Supporting Information S1

Correspondence to:
C. P. Gabrielli,
chris.gabrielli@usask.ca

Citation:
Gabrielli, C. P., & McDonnell, J. J. (2018). No direct linkage between event-based runoff generation and groundwater recharge on the Maimai hillslope. *Water Resources Research*, *54*, 8718–8733. https://doi.org/10.1029/2017WR021831

Received 14 SEP 2017
Accepted 9 OCT 2018
Accepted article online 19 OCT 2018
Published online 8 NOV 2018

No Direct Linkage Between Event-Based Runoff Generation and Groundwater Recharge on the Maimai Hillslope

C. P. Gabrielli[1] **and J. J. McDonnell**[1,2]

[1]Global Institute for Water Security, University of Saskatchewan, Saskatoon, Saskatchewan, Canada, [2]School of Geography, Earth and Environmental Sciences, University of Birmingham, Birmingham, UK

Abstract Hillslope hydrological investigations in humid regions to date have focused mostly on runoff generation during events. The few papers that have also examined groundwater recharge processes associated with subsurface stormflow production have found strong linkages between episodes of runoff and recharge to the aquifer. But the range of climate, vegetation, and geological conditions examined thus far has been limited. Here we explore how geologic characteristics, timing of subsurface stormflow, and hydroclimatic conditions relate to the timing of bedrock groundwater recharge at the well-studied Maimai watershed. We hypothesized that recharge would be determined by subsurface stormflow frequency in this system with high rainfall and little seasonality of the hydrologic response. Unexpectedly, isotopic analysis and noble gas measurements indicated that recharge occurred almost exclusively during winter months despite previous work at Maimai showing subsurface stormflow occurs in all seasons and rainfall-runoff ratios are high year-round. A sprinkler and dye experiment conducted directly on open bedrock identified groundwater recharge mechanisms and rates, and a simple empirical recharge model suggests almost 90% of recharge occurred from only 55% of annual precipitation. We found no correlation between the timing and magnitude of groundwater recharge and total precipitation, direct runoff or subsurface stormflow. The catchment effectively converted rainfall to runoff during all seasons, but the unfractured low permeability bedrock (2.3×10^{-8} m/s) required long durations of extended catchment wetness for appreciable recharge to occur—a condition satisfied only during winter months with lower evapotranspiration. These findings suggest the need to better understand the geologic controls of recharge in headwaters.

1. Introduction

Most of the early hillslope hydrology work focused on event-scale streamflow generation processes (i.e., lateral flow) through the often thin veneer of soil covering these hillslopes (Harr, 1977; Hewlett & Hibbert, 1967; Mosley, 1979; Sklash & Farvolden, 1979). And since then, many of the key studies (Ali et al., 2011; Jencso & Mcglynn, 2011; Tetzlaff et al., 2014; Wienhöfer & Zehe, 2014) have followed this same focus in new locations around the world, documenting the many factors responsible for lateral flow domination (Bachmair et al., 2012), including key combinations of slope angle, slope length, soil depth, and bedrock permeability (Hopp & Mcdonnell, 2009). While the factors for subsurface stormflow production are now reasonably well understood across diverse systems—all collapsing into some form of filling, spilling, transmission losses, and then whole-slope runoff activation thresholds (Ameli et al., 2015; Jackson et al., 2016; Mcdonnell, 2013)—recharge processes, defined as percolation of water below the rooting zone to the deeper underlying headwater aquifer, have received considerably less attention. The studies that have looked at groundwater recharge on hydrologically active hillslopes (i.e., ones that yield measureable subsurface stormflow) have shown a direct connection to times of subsurface stormflow initiation and recharge to the aquifer below. For example, Buttle and Mcdonald (2002) showed that event-scale groundwater recharge at an Ontario hillslope was 34–41% of total groundwater recharge through the year. Similarly, Graham, Van Verseveld, et al. (2010) showed for a hillslope at the H.J. Andrews Experimental Forest in Oregon that 41% of annual groundwater recharge occurred during events that yielded subsurface stormflow. For sites in Japan, Kosugi et al. (2006) showed that 55% of groundwater recharge occurred during storm events, and lastly, model analysis of hillslope groundwater recharge by Appels et al. (2015) showed at the Panola hillslope site that 40% of annual recharge occurred during events that generated subsurface stormflow. Runoff ratios on these same slopes have ranged from 3.5% to 43% (Kosugi et al., 2006; Peters et al., 1995; Tromp-Van Meerveld &

Mcdonnell, 2006; Woods & Rowe, 1996). Field study (Asano et al., 2002) and model analysis (Ebel & Loague, 2006; Hopp & Mcdonnell, 2009) have shown that this ratio depends mainly on bedrock permeability, soil depth, and slope angle. Additionally, the spatial variability of bedrock permeability and soil thickness can cause high spatial variability in recharge on the slope, with greater recharge found in bedrock depressions where filling and spilling occurs (Appels et al., 2015).

While these and other recent efforts have begun to tackle questions of groundwater recharge on steep slopes that generate significant lateral flow, few studies have examined the detailed hydrogeologic conditions through the weathered and unweathered unsaturated critical zone above the water table and below the soil-bedrock interface that are key to a complete mechanistic assessment of bedrock recharge (as noted recently by Grant and Dietrich, 2017). Here we define bedrock as all material below the soil profile, including saprolite and weathered bedrock. One-dimensional lysimeter experiments aimed at groundwater recharge abound in the literature (Heppner et al., 2007; Kendy et al., 2003; Wu et al., 1996). However, few studies have quantified such rates on real hillslopes. Of course, a very large literature exists at larger catchment and large aquifer scales regarding the seasonal, interannual, and intra-annual variability in groundwater recharge (Blöschl et al., 2017; Jasechko et al., 2014; Petersen et al., 2012). These studies have shown that the temporal variability of precipitation, as well as temporal variations in the partitioning of precipitation to water balance components, primarily evapotranspiration (ET; Milly, 1994), has a large effect on when recharge occurs. Regional hydroclimatic patterns such as synchrony between precipitation (*P*) and ET exerts strong controls on both runoff (Berghuijs et al., 2014) and recharge (Xu & Chen, 2005). Where winter rainfall (or winter snowfall with associated spring freshets) occur, groundwater recharge is often highly seasonal (O'driscoll et al., 2005). This is in contrast to regions where *P* and ET are more in sync, for which storm size and rainfall intensity can act as the primary control of recharge magnitude and timing (Milly, 1994; Tang & Wang, 2017).

So between the extremes of the point scale lysimeter work and large catchment and aquifer scale work, it is still unclear how hillslope hydrogeologic structure influences the timing of deeper recharge processes—beyond the simple association between subsurface stormflow production and initiation of deep groundwater recharge. Hillslope-scale irrigation experiments (Brooks et al., 2004; Graham, Van Verseveld, et al., 2010; Jackson et al., 2016; Tromp-Van Meerveld et al., 2007; Van Verseveld et al., 2017) have shown generally that bedrock properties influence subsurface stormflow dynamics and the hillslope water balance, but how these bedrock characteristics influence the mechanisms that control the proportion of deep recharge (and the timing of its activation) is still poorly understood. Many process questions still remain: What conditions are required to initiate bedrock groundwater recharge in the headwaters? What are the spatial and temporal patterns of these conditions? How do soil and bedrock characteristics work in concert (or in opposition) for deep recharge generation? And how is total recharge magnitude and timing set by interactions between hydroclimate seasonality and critical zone conditions?

Here we conduct a field-based investigation of hillslope and catchment groundwater recharge at the well-characterized Maimai watershed. We build on Mcdonnell (1990), Woods and Rowe (1996), and Mcglynn et al. (2002). These previous studies (and many more, dating back to Mosley, 1979) have Shown That subsurface stormflow on the steep Maimai slopes occurs in all seasons and above a rainfall threshold (generally) of 20 mm (Graham, Woods, & Mcdonnell, 2010). Long-term data between 1975 and 1987 show that there were 710 storm events with precipitation greater than 6 mm. Of these 710 events, 460 exceeded the 20-mm threshold for subsurface stormflow production—equal to 65% of all events—225 of which (49%) occurred in the summer (November–April) and 235 of which (51%) occurred in the winter (May–October). Based on this, we hypothesized that hillslope-scale groundwater recharge is controlled largely by event inputs that generate subsurface stormflow. And given the unusually high frequency and unusually low seasonality in the occurrence, magnitude, and duration of events that cause subsurface stormflow, seasonality of groundwater recharge at Maimai was expected to be limited based on the past associations at other sites between subsurface stormflow production and groundwater recharge.

We present a forensic hillslope analysis where we removed the hillslope soil mantle across a 10.5-m^2 slope section above the former Woods and Rowe (1996) hillslope and conducted a 96-hr sprinkler experiment to determine bedrock surface infiltration characteristics and to determine its role in redistributing

water to depth. Finally, we drilled the critical zone down to 9 m at 40 locations across the 4.5-ha catchment to explore the depth and hydraulic characteristics of the unsaturated bedrock above the water table and below the soil-bedrock interface. Recent work by Gabrielli et al. (2018) has shown that the spatial extent, dynamics, and age of the groundwater in the underlying bedrock aquifer at Maimai, as well as its contribution to streamflow and influence of streamwater age, are controlled by bedrock permeability. We also present new noble gas recharge temperature (NGT) data, groundwater isotopic composition, and long-term climate and runoff data to explore directly the hillslope-scale groundwater recharge processes at the steep, wet Maimai site. We also combined our intensive field campaign with a simple modeling exercise to test our hypothesis that episodes of subsurface stormflow drive groundwater recharge. In so doing, we connect and synthesize a number independent data sets to establish a coherent description of hillslope-scale subsurface hydrologic partitioning. The following specific questions guide the flow of the paper and our findings at the Maimai hillslope:

1. How do bedrock characteristics control recharge mechanisms?
2. When does groundwater recharge occur on steep hillslopes?
3. How does the soil mantle affect the recharge process?
4. How does the study hillslope compare to other highly monitored sites elsewhere in terms of the timing, frequency and duration of bedrock groundwater recharge?

2. Study Site

The Maimai watershed is located approximately 15 km inland from the northwest coast of the South Island of New Zealand (Figure 1; 42°05′S 171°47′E). The highly dissected landscape is defined by its short steep slopes and thin soils. Hillslope lengths average less than 50 m and the average slope is 34° with short sections nearing 55°.

The wet temperate coastal environment receives, on average, 2,600 mm of rainfall annually with nearly 150 rain days per year. Frontal systems from the Tasman Sea produce long duration, low-intensity storms, with average rainfall intensities of ~1.2 mm/hr, although storms have produced short-term intensities upward of 30 mm/hr. It is not uncommon for total rainfall to exceed 100 mm for single events. There is only slight seasonality in rainfall with midwinter months (July–August) being slightly wetter than midsummer (January–February) months (412 vs. 318 mm, respectively). The low catchment elevation and proximity to the coast result in only one to two snow days each year, which melt within hours to days.

The constant rainfall results in persistent high antecedent moisture conditions and a soil mantle that is believed to rarely drop below 10% of saturated water content (Mosley, 1979). The catchment is defined by its highly responsive and flashy storm hydrograph and an annual runoff ratio of ~60% that is among the highest of any research catchment reported in the literature (Anderson & Mcdonnell, 2005). Approximately 1,000 mm (65%) of the 1550 mm of average annual runoff leaves the catchment as quick flow, as defined by the Hewlett and Hibbert (1967) separation method (Mcdonnell, 1990).

Soils are thin (range: 0.1–1.8 m, average: 0.6 m) and broadly classified as Blackball Hill soils (Mcdonnell, 1990). They are characterized as podsolized to mottled yellow-brown earths along the hillslopes and ridges and gley soils within the poorly drained hollows and riparian zones. Infiltration capacity in the top 170-mm humic horizon is as high as 6,100 mm/hr and average hydraulic conductivity of the upper mineral soil is on the order of 250 mm/hr (Mcdonnell, 1990).

The bedrock underlying the catchment is known as Old Man Gravel belonging to a larger formation known as the Old Man Group (Bowen, 1967), which was laid down in the early Pleistocene as a thick (>400 m) layer of glacial outwash during an erosional sequence in the formation of the Southern Alps (Mortimer et al., 2001). The bedrock is a conglomerate composed primarily of sandstone clasts (greywacke) with small additions of schist and granite in a compact weakly cemented sandy-clay matrix. The rounded clasts range in size from 10 to 500 mm in diameter but are mostly less than 200 mm in diameter (Mortimer et al., 2001).

This research is focused primarily in the 4.5-ha M8 subcatchment (Figure 1a) within the Maimai watershed. Landscape structure, geology, soil, and runoff characteristics in the M8 subcatchment are similar to those of the other subcatchments within the larger Maimai Experimental Watershed (Mcglynn et al., 2004). Total

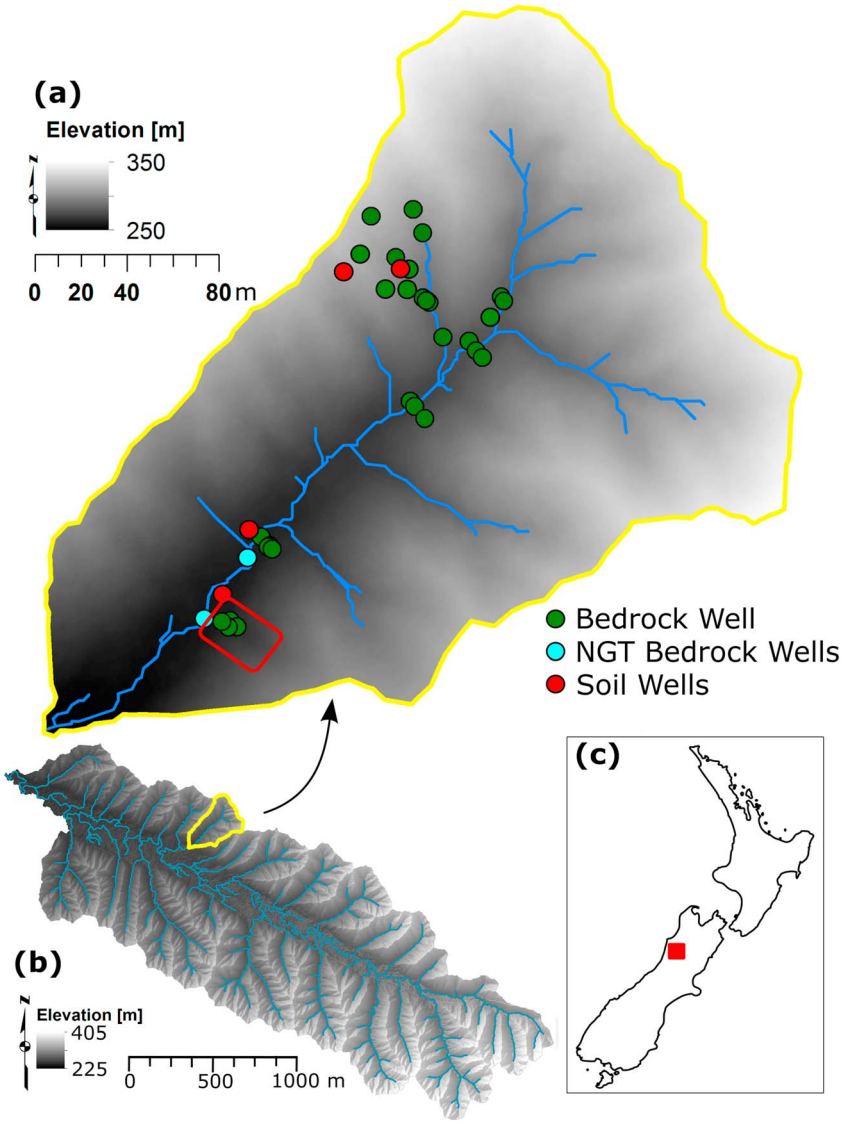

Figure 1. (a) M8 subcatchment with location of bedrock and soil wells, as well as the two wells sampled for noble gas recharge temperature (NGT) analysis. The red rectangle indicates the general region of the landslide scar and sprinkler experiment. (b) Maimai Experimental Watershed and (c) New Zealand locational inset.

catchment relief in M8 is approximately 100 m with elevations ranging from 250 to 350 m above sea level. For a review of previous research at M8, see Mcglynn et al. (2002).

3. Data and Methods

Our study approach starts by defining bedrock characteristics and the mechanism of bedrock groundwater recharge through borehole testing and a plot-scale sprinkler experiment. Groundwater measurements of noble gas and stable isotopes of water were then used to identify seasonality in bedrock recharge. We quantified seasonal fluctuations in hydroclimatic forcing that drive catchment wetness conditions to identify correlations with temporal patterns of recharge. To explore intra-annual and interannual patterns of bedrock recharge timing and volume, we constructed a simple empirical recharge model constrained by known the mean annual recharge magnitude and temperature and relate our findings to seasonality of various hydroclimatic metrics over the 13-year period from 1975 to 1987. We finished by running the model for an additional 1-year period during the 2015 calendar year and compared results to daily soil water data to

further identify linkages between catchment wetness patterns, soil water dynamics, runoff characteristics, geologic structure, and the seasonality of recharge.

3.1. Bedrock Characteristics and Recharge Mechanisms

3.1.1. Hydraulic Conductivity

Forty bedrock wells were drilled within the M8 catchment across the four major landscape units: the riparian zone, toe slopes, hillslopes, and ephemeral hollows. Bedrock saturated hydraulic conductivity (Ksat) was calculated as the geometric mean for each landscape positions following the Hvorslev (1951) approach using falling-head slug tests, as outlined in Gabrielli et al. (2018). We observed an abrupt contrast in hardness immediately below the soil column that refused penetration with a hand auger. This sharp boundary was observed at all landscape positions drilled within the catchment.

3.1.2. Sprinkler Experiment: Bedrock Infiltration Rate and Mechanisms of Recharge

We conducted a plot-scale sprinkler experiment on an exposed section of bedrock to identify the flow mechanisms associated with bedrock groundwater recharge and to test plot-scale bedrock infiltration rates. We specifically sought to distinguish between recharge by bedrock fracture flow (defined here as the secondary porosity of the bedrock) and recharge by diffuse matrix flow within the porous rock structure (defined here as the primary porosity of the bedrock). We expected these different mechanisms of bedrock recharge to be associated with different catchment wetness conditions.

The sprinkler experiment was conducted on a previously trenched and instrumented planar hillslope just downstream of the main M8 catchment weir (Graham, Woods, & Mcdonnell, 2010; Woods & Rowe, 1996). A small landslide occurred in 2013 on the hillslope removing the overlying colluvium down to the soil-bedrock interface over an area of approximately 300 m^2 (30 m upslope by 10 m across slope—see Figure 1 for general location). We constructed a 150-mm-tall cement berm around the landslide scar to isolate and collect surface runoff from within the landslide area.

Water was pumped from a 200-L stilling basin through a sprinkler system onto the open bedrock surface wetting an area of 10.5 m^2 at the toe of the landslide scar. Surface runoff was collected and routed back to the stilling basin creating a closed loop system. Once the initial bedrock surface storage was filled, bedrock infiltration and surface evaporation represented the only withdrawal of water from the system. To separate bedrock infiltration from evaporative loss, we assumed no evaporation between the hours of 22:00 and 06:00. We operated the sprinkler continuously for 96 hr, providing four nights of measurements. In traditional sprinkler experiments where prescribed rainfall rates rarely exceed the soil infiltration capacity, large volumes of input water are required along with precise control of pumping and sprinkler rates. These requirements have historically made field-based sprinkler experiments logistically difficult to perform. However, our site's absence of soil, low bedrock infiltration rates, and the recollection of applied sprinkler water allowed for a simple and novel implementation of the traditional sprinkler experiment. Because the rainfall application rate was much greater than bedrock infiltration, excess surface water was always present at the bedrock surface. This condition made it possible to relax the need for exact control or knowledge of sprinkling rates, considerably simplifying the field design.

Bedrock infiltration was determined by fitting a linear regression to stilling basin water level measurements for each night (recorded using a capacitance-type water level logger (Odyssey®) at 10-min intervals). The slope of the regression line (L/T) multiplied by the surface area of the stilling basin (L^2) equaled the volumetric loss rate of water from the system (L^3/T) into the bedrock. We averaged the regression line slopes from the four nights to create a master slope. Finally, this average volumetric loss rate was divided by the wetted bedrock area to determine the plot-scale bedrock infiltration rate.

Additionally, we conducted tracer and hydrometric analysis to identify bedrock flow paths and to distinguish between fracture and matrix flow. We recorded water table elevation in two bedrock wells, one located within the wetted area and one immediately downslope, to capture rapid infiltration of sprinkler water to the water table if present. Brilliant blue dye and a salt slug were added to the sprinkler water at hour 48. We monitored bedrock groundwater electrical conductivity prior to, during, and for 120 hr after the sprinkler experiment, to identify the breakthrough curve of infiltrating water. Finally, we destructively sampled and analyzed the bedrock surface at the end of the experiment with a diamond blade chain saw to identify bedrock flow paths via visual observations of the depth of dye penetration and degree of bedrock fracturing.

3.2. Recharge Seasonality

3.2.1. Noble Gas Measurements

We analyzed gas concentrations in groundwater samples taken from two bedrock wells located in the toe slope and riparian zone within the lower part of the M8 catchment to determine NGT (Lindsay, 1979; Niu et al., 2017; Figure 1). NGT reflects environmental conditions during seasonally focused recharge periods and provides a means to directly identify seasonal patterns in groundwater recharge by matching NGT values to seasonal temperature variations. Samples were collected under deep baseflow conditions and three well volumes were evacuated from each well prior to sampling. Dissolved argon (Ar) and nitrogen (N_2) were measured in both samples at the Institute of Geological and Nuclear Sciences Stable Isotope Laboratory (Lower Hutt, New Zealand), and NGT was determined using the standard graphical method (Bohlke & Krantz, 2003; Heaton & Vogel, 1981).

3.2.2. Stable Isotope Measurements

We used the possible existence of a seasonal contrast in isotopic composition between soil and bedrock groundwater to further test for seasonal bedrock groundwater recharge. Soil water mean residence time was previously established at less than 4 months for the M8 catchment (Stewart & Mcdonnell, 1991). Late summer soil water was therefore expected to heavily reflect the isotopic composition of summer precipitation. Due to simple temperature driven fractionation, bedrock groundwater was expected to have an isotopic composition distinctly more depleted than late summer soil water if recharge was sourced primarily from colder winter soil water (Kendall & Mcdonnell, 1998).

We collected soil, surface, and bedrock groundwater samples for isotope analysis over three sampling periods all under summer low flow conditions: 16 January 2015, 1 February 2015, and 24 February 2015. Streamwater was collected at the catchment outlet during each sampling period, and different soil and bedrock wells were sampled for each of the three periods. Samples collected during the first two periods were stored in 30-ml glass scintillation vials and sealed with parafilm. Samples were analyzed at the University of Saskatchewan using a Los Gatos Research liquid water isotope analyzer that utilizes high-resolution laser absorption spectroscopy. Analytical precision was ±0.2‰ for ^{18}O and ± 1.0‰ for ^{2}H. Samples from 24 February 2015 were analyzed for ^{18}O and ^{2}H at the Institute of Geological and Nuclear Sciences Stable Isotope Laboratory. Samples were analyzed using a GV Instruments Isoprime mass spectrometer coupled with a PyrOH elemental analyzer. Analytical precision was ±0.1‰ for ^{18}O and ± 1.0‰ for ^{2}H.

3.3. Climatic and Hydrologic Seasonality

To identify seasonality in climate and hydrologic metrics, we used long-term rainfall-runoff records from the M8, as well as publically available data from a meteorological station maintained by the New Zealand National Institute of Water and Atmospheric Research located in the township of Reefton, 5 km west of Maimai (latitude: −42.11578, longitude: 171.86014).

Daily rainfall (P) and catchment discharge (Q_{tot}) were measured at M8 from 1975 to 1987. Rainfall was recorded using a tipping bucket rain gauge located 500 m from the M8 outlet, and M8 discharge was recorded with a 90° v-notch weir located within M8. We also calculated baseflow (Q_{base}) using a recursive digital filter on 1-hr discharge data via the WHAT hydrograph analysis tool (Lim et al., 2005). Direct runoff (Q_{dir}) was calculated as total runoff minus baseflow ($Q_{tot} - Q_{base}$). We used daily temperature records (T) from the Reefton meteorological station to calculate potential evapotranspiration (PET) from 1975 to 1987 using the Thornthwaite (1948) approach. Monthly averaged T, P, Q_{tot}, Q_{base}, Q_{dir}, and PET over the 13-year monitoring period were used to identify intra-annual hydroclimatic seasonal patterns.

3.4. Bedrock Groundwater Recharge Model

We constructed a simple empirical recharge model combined with a temperature-based mass balance to explore temporal patterns of bedrock groundwater recharge over the 13-year period from 1975 to 1987. We used inverse modeling to constrain model output to known observations of annual bedrock groundwater recharge magnitude and temperature. We then compared the resulting temporal pattern of recharge to the hydroclimatic variables described above. Finally, we modeled bedrock groundwater recharge for the year 2015 and compared model output to daily soil water data from wells in the soil (0.15- to 1.8-m depths below soil surface) in the four main landscape positions to further elucidate the temporal linkages between catchment storage conditions, soil water states, and bedrock recharge. Modeling and analysis time periods were

Table 1
Landscape Position and Mean Saturated Hydraulic Conductivity (Ksat) Values for the 40 Bedrock Wells Tested Through Falling-Head Slug Tests

Landscape unit	Number of wells	Geometric mean Ksat (m/s)
Hillslope	13	2.3×10^{-8}
Hollow	10	1.4×10^{-7}
Toe slope	6	2.9×10^{-6}
Riparian	11	6.6×10^{-5}

limited by data availability. Long-term runoff and hydrometric data were only available for the 1975–1987 period, while time series of soil moisture were only available for calendar year 2015. Full model description is provided in the supporting information. Note that we use this simple modeling exercise not to identify or capture exact physical processes of groundwater recharge or bedrock infiltration but instead to identify how seasonal patterns of recharge might be associated with seasonal precipitation, ET, storage, and wetness conditions and to understand how bedrock characteristics might affect these associations.

4. Results

4.1. Mode of Recharge: Bedrock Sprinkler Experiment and Bedrock Characterization

4.1.1. Bedrock Characterization

Spatial patterns of bedrock saturated hydraulic conductivity (Ksat) largely followed the main geomorphic landscape units within the catchment. Although considerable variability existed within each landscape unit, mean saturated hydraulic conductivity increased from hillslope to hollow to toe slope to the riparian zone. Geometric mean values, respectively, were 4.47E−08, 8.27E−07, 3.27E−06, and 1.08E−05 m/s (Table 1).

4.1.2. Sprinkler Experiment

During the 96-hr sprinkler experiment an equivalent rainfall depth of 4,950 mm, or approximately 2 years of rainfall, was applied to the 10.5-m^2 open bedrock surface. Figure 2 shows the water level time series from the stilling basin during the sprinkler experiment. Linear regression models fit well to water table drawdown data for each night (R^2: 0.99, 0.97, 0.99, and 0.98 for nights 1–4, respectively), indicating a relatively constant rate of bedrock infiltration through each evening. Water loss from the stilling basin ranged from 0.70 to 3.97 L/hr and averaged 2.2 ± 1.17 L/hr, corresponding to an average bedrock infiltration rate of 5.69E−08 ± 3.09E−8 m/s. The sprinkler-based mean bedrock infiltration rate corresponded well to the geometric mean Ksat of hillslope bedrock tested via slug tests (Table 1) and also to previous measurements at the site (Gabrielli et al., 2012;

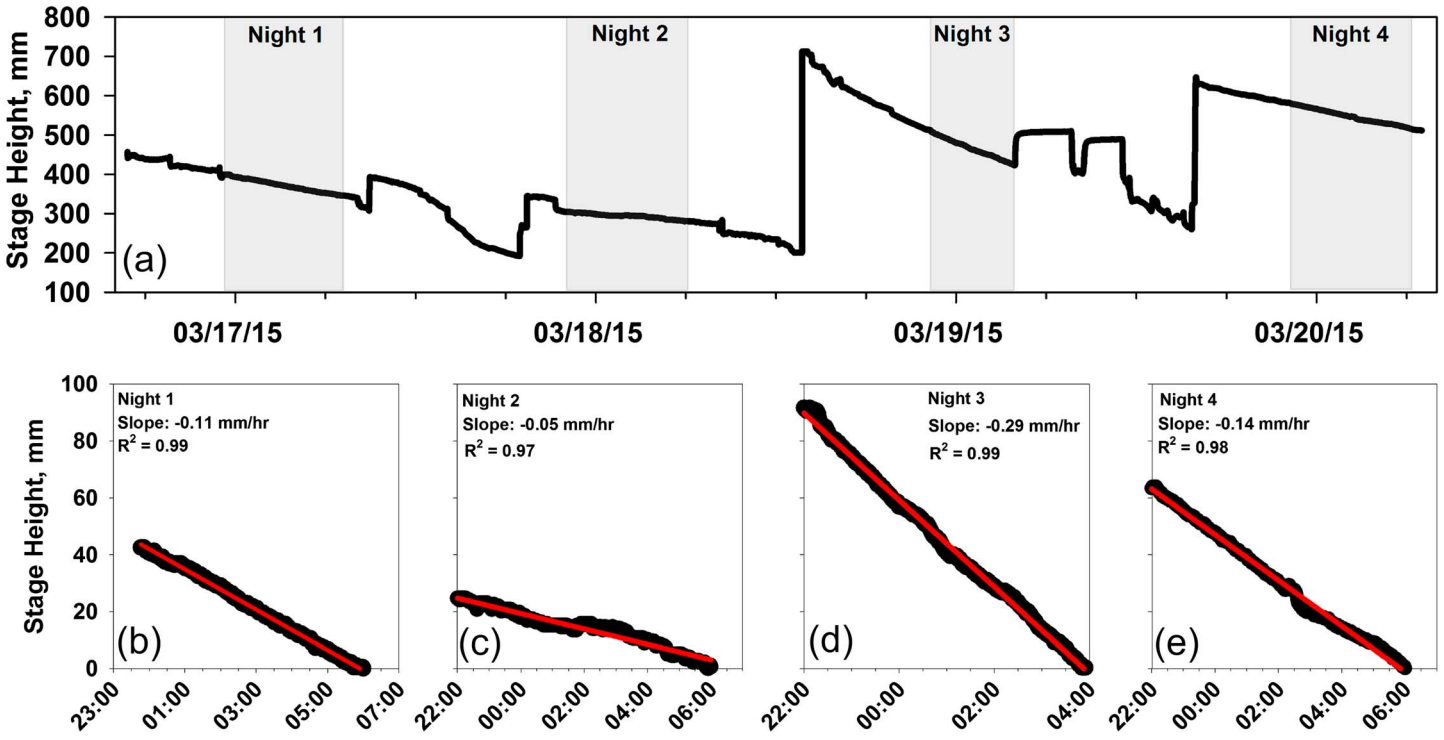

Figure 2. (a) Stage height time series of sprinkler stilling basin with highlighted sections showing data from each night and (d–e) selected stage data with fitted linear regression.

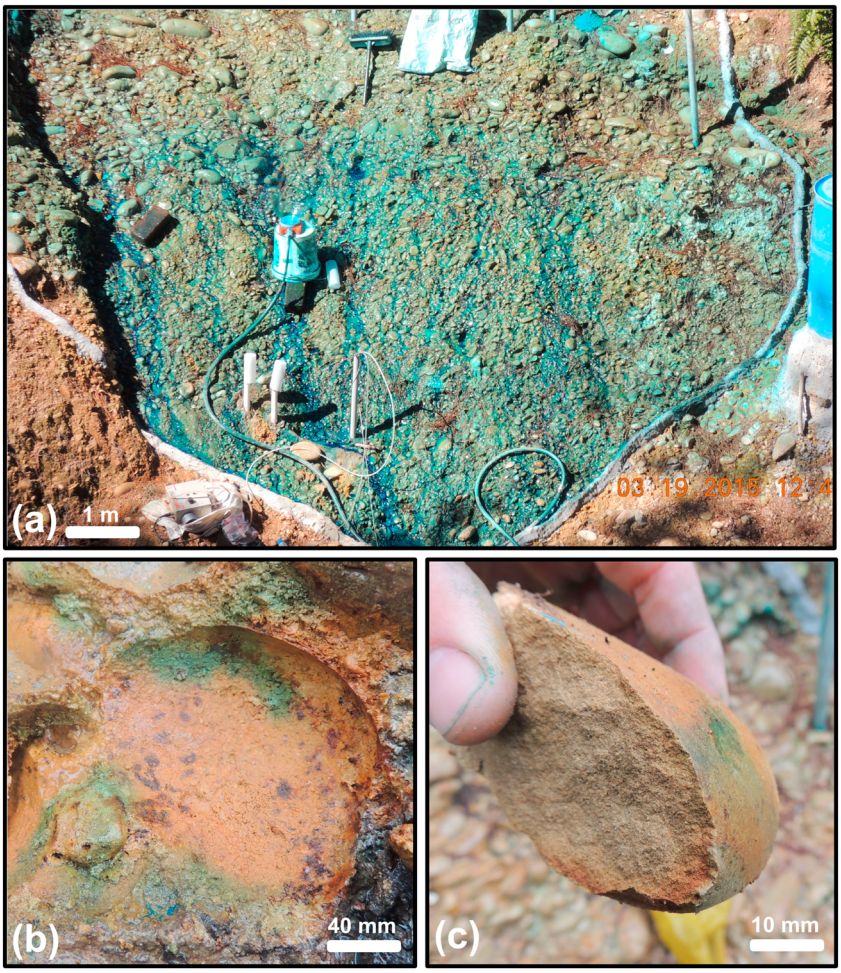

Figure 3. (a) Bedrock sprinkler experiment showing brilliant blue dye staining of the bedrock surface and the extent of the sprinkler plot (b) Destructive testing of the bedrock surface post sprinkler experiment—here a sandstone clast has been removed from the bedrock surface revealing (minimal) preferential flow between the clast-matrix boundary. This preferential flow did not extend beyond the depth of surface clasts. (c) A surface clast freshly split revealing no dye penetration within the clast.

Graham, Woods, & Mcdonnell, 2010). Destructive analysis of the bedrock surface revealed no evidence of fracture pathways within the upper zone of the bedrock across the wetted and dyed area (Figure 3a). Dye infiltration was minimal overall but did show a tendency (visually) toward preferential flow along the boundaries between clasts and matrix. The embedded and isolated nature of most clasts within the matrix, however, prevented these preferential flow paths from connecting to deeper zones and these flow paths occurred only for clasts found within the surface layer of the bedrock (Figure 3b). No vertical penetration of dye beyond 5–10 mm was noted within the bedrock matrix. This is consistent with the 0.2-mm/hr infiltration rate calculated during the experiment. Thirty clasts from 10 locations on the slope were split immediately after the experiment to look for dye penetration. No dye penetration was found in any of these clasts (Figure 3c). Taken together, these observations suggest a general lack of fracturing or fracture flow paths within the bedrock, inferring that bedrock recharge likely occurs exclusively as porous media flow through the bedrock matrix.

Bedrock water table dynamics and electrical conductivity in observation wells remained unchanged during and for the 120-hr postexperiment observation period (data not shown), further confirming a general absence of rapid flow paths through the bedrock. The lack of changes in the water table and electrical conductivity values also indicated that no direct recharge reached the underlying bedrock water table during the observation period via matrix flow or otherwise, consistent with the measured Ksat and time length of the experiment.

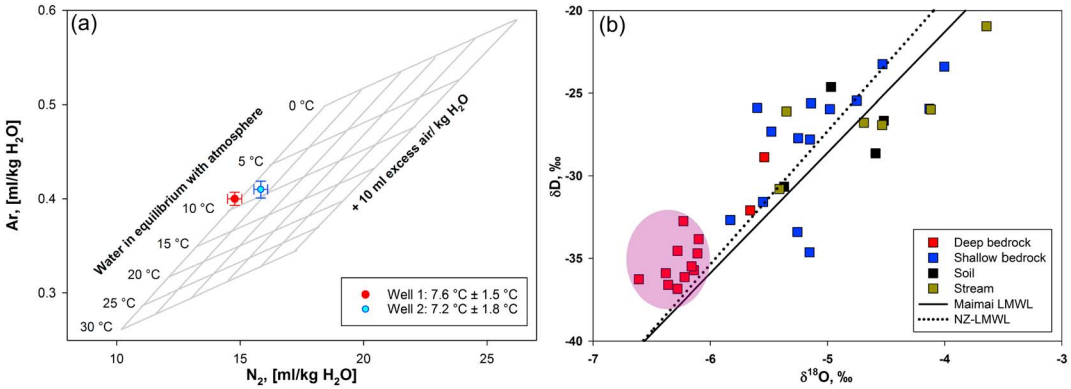

Figure 4. (a) Dissolved nitrogen and argon concentrations of well samples overlaid on grid showing atmospheric equilibrium concentration and in the presence of excess air, figure style (cf. Heaton & Vogel, 1981). (b) Dual isotope plot of groundwater samples from deep bedrock, shallow bedrock, and soil wells in addition to streamwater samples and Maimai and New Zealand local meteoric water lines (LMWL). The shaded region shows the distinctly more negative isotopic signature of the deep bedrock wells, suggesting bedrock groundwater recharge from cold-season precipitation.

4.2. Bedrock Groundwater Recharge Seasonality

We determined groundwater recharge temperatures of 7.6 ± 1.5 °C for bedrock well 1 and 7.2 ± 1.8 °C for well 2 (Figure 4a). These NGTs represent the mean volume-weighted annual recharge temperature of the sampled water. Under conditions of uniform monthly recharge, NGT would equal the local mean annual air temperature of 11.3 °C, nearly 4 °C warmer than observed recharge temperatures. Additionally, mean summer temperature from November to April was 14.8 °C, and mean winter temperature from May to October was 7.8 °C. The similarity between NGT values and mean winter air temperatures reveals a strong seasonal bias in bedrock groundwater recharge toward colder months indicating bedrock groundwater recharge is sourced primarily from winter season precipitation.

Isotopic composition of the sampled summer stream, soil, and bedrock groundwater ranged from −6.61‰ to 4.53‰ $\delta^{18}O$ and −36.85‰ to −23.25 ‰ δD (Figure 4b). A cluster of bedrock groundwater samples from deep upper-hillslope wells and from identified groundwater discharge zones within the lower riparian corridor had distinctly depleted isotopic compositions compared to all other streamwater, soil water, and shallow bedrock groundwater samples. The distinct isotopic signature of the deeper bedrock groundwater in comparison to other catchment waters provides evidence of recharge to the bedrock aquifer from waters associated with precipitation *outside* of the summer season. The relative depletion of the isotopic signature further supports cold-season precipitation as the source of bedrock groundwater recharge.

4.3. Bedrock Groundwater Recharge Model

Daily modeled bedrock groundwater recharge was calculated using a least squares parameter fitting routine which best captured mean annual recharge totals and mean annual recharge temperature over the modeling period from 1975 to 1987. Daily values were averaged to monthly and compared with hydrologic and climate variables.

4.3.1. Seasonal Patterns of Recharge and Hydroclimatic Variables

Mean monthly modeled recharge is displayed in Figure 5, along with long-term mean monthly P, Q_{tot}, and PET from 1975 to 1987. Recharge followed a clear seasonal trend peaking at nearly 34 mm/month in July during midwinter and dropping to near zero throughout most of the summer. PET followed a similar but inverse seasonal pattern, peaking during the summer and declining considerably during the colder winter months. Precipitation and runoff were slightly lower from February to April but showed little seasonality otherwise. Sixty percent of annual recharge occurred during the months of June, July, and August that delivered only 25% of the annual precipitation and nearly 90% of annual recharge occurred during the 6-month period from May to October, during which 55% of annual precipitation fell.

We tested correlations between bedrock recharge and various rainfall and catchment runoff metrics to elucidate the magnitude and temporal characteristics associated with the redistribution of rainfall inputs

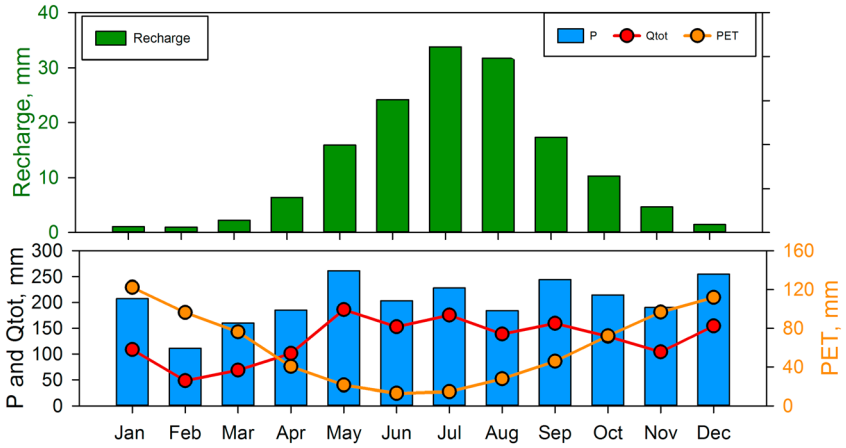

Figure 5. (top) Mean monthly modeled bedrock groundwater recharge. (bottom) Total catchment discharge (Q_{tot}) and potential evapotranspiration (PET). All monthly values were averaged from daily values between 1975 and 1987.

between runoff and recharge (Figure 6 and Table S1). As expected, rainfall and total catchment runoff were highly correlated (Figure 6a, R^2 = 0.81). The catchment rainfall-runoff ratio averaged 60% annually and was slightly higher during the winter (71%) compared to summer (51%) indicating slightly more efficient conversion of rainfall inputs to runoff during cold-season intervals. Further, direct runoff (Q_{dir}) as a proportion of total runoff (Q_{tot}) was extremely high and showed little seasonality (coefficient of variation: 0.03). This ratio averaged 0.77 annually, suggesting event rainfall inputs were efficiently converted to storm runoff irrespective of time of year. Despite the seasonally constant rainfall and runoff, monthly rainfall and recharge were almost completely uncorrelated (Figure 6b, R^2 = 0.09), indicating that monthly rainfall totals were a poor predictor of monthly recharge. This general lack of correlation also existed

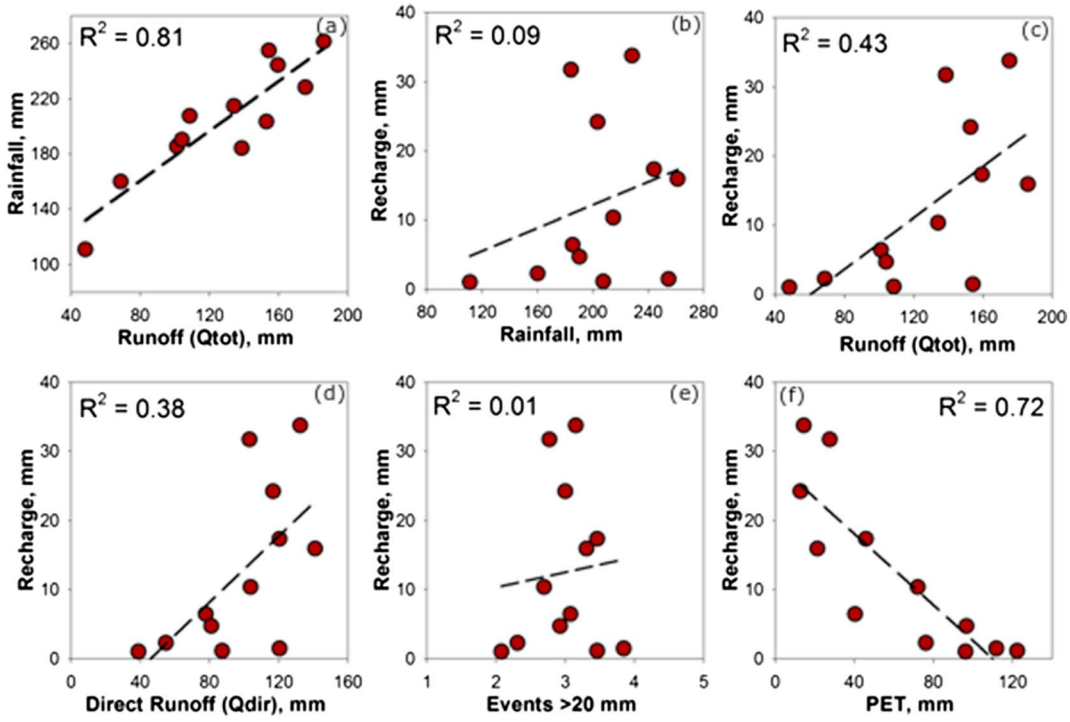

Figure 6. (a–e) Mean monthly recharge versus P, Q_{tot}, Q_{dir}, Q_{base}, and PET and (f) rainfall versus runoff. All monthly values were averaged from daily values between 1975 and 1987.

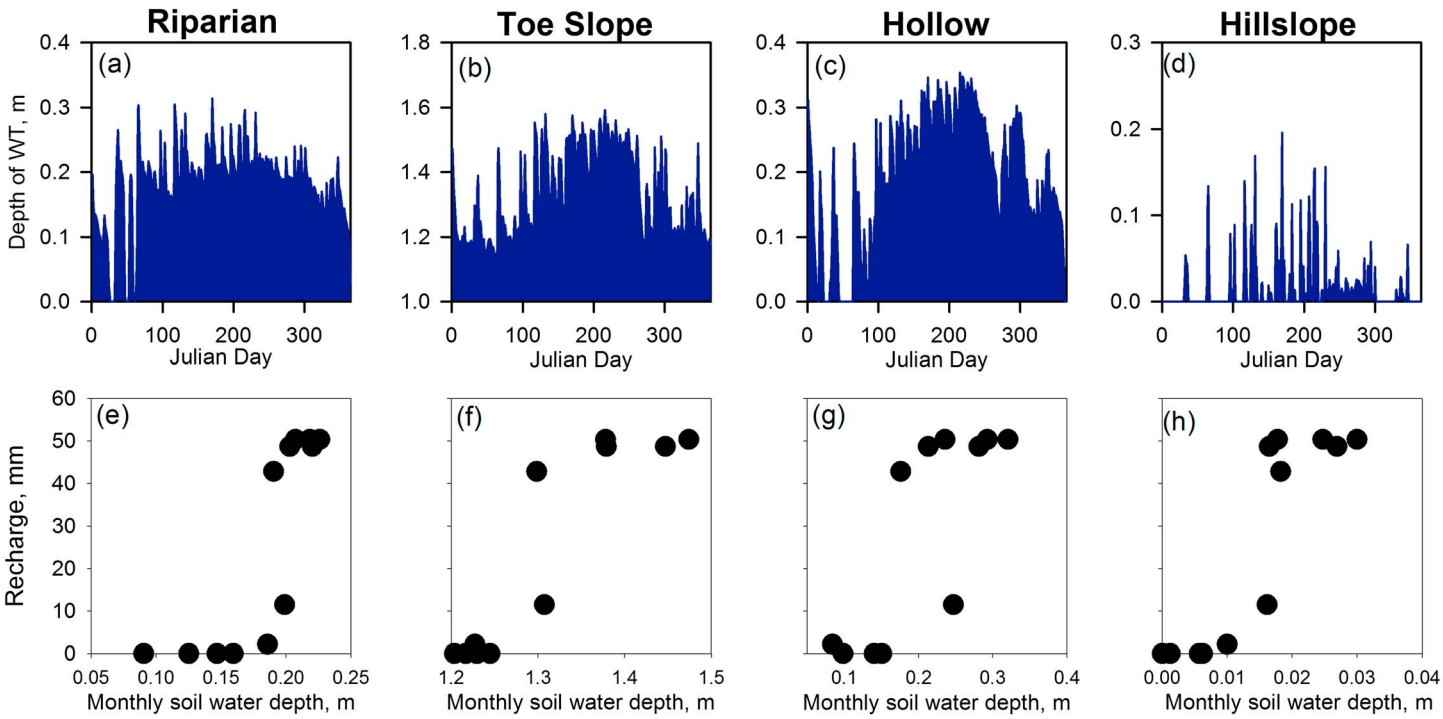

Figure 7. (a–d) Depth of water table above the soil-bedrock interface for four soil wells located in riparian, toe slope, hollow, and hillslope positions. (e–h) Modeled bedrock groundwater recharge compared to monthly mean depth of water table for each soil well for the year 2015.

between bedrock recharge and total runoff (Figure 6c, $R^2 = 0.43$) and direct runoff (Figure 6d. $R^2 = 0.38$). We calculated the average number of rainfall events per month exceeding the 20-mm subsurface stormflow initiation threshold for the 13-year period between 1975 and 1987 and regressed this against average monthly recharge (Figure 6e) and found no correlation either ($R^2 = 0.01$), further reinforcing the lack of relationship between runoff processes and recharge at Maimai. Monthly recharge, however, was strongly correlated to monthly PET (Figure 6f, $R^2 = 0.72$), suggesting that seasonal patterns of recharge tracked well with inverse seasonal patterns of catchment evaporation.

4.3.2. Soil Water Comparison

Figures 7a–7d show the 2015 time series of daily mean water table depth above the soil-bedrock interface for each of the four monitored soil wells. The riparian, toe slope, and hollow wells were perennially saturated but showed a distinct and sustained water table rise during the winter season. The hillslope well (Figure 7d) had a transient water table that occurred with greater consistency during the winter months, which also existed during larger storms throughout the summer season. Figures 7e–7h display the 2015 mean monthly water table depth for each well plotted against modeled mean monthly bedrock recharge for the same time period. A strong threshold-like relationship was observed such that below a mean water table depth (specific to each well), little to no recharge occurred, but above that threshold monthly recharge increased to, and sustained, a constant rate.

5. Discussion

Our results suggest the complex interactions between bedrock characteristics, soil storage, and seasonal climatic conditions at Maimai control bedrock groundwater recharge timing and magnitude. But unlike past hillslope studies elsewhere, we found no clear direct linkage between hillslope-scale bedrock groundwater recharge and rainfall events. Maimai receives 2,600 mm of precipitation annually with minimal seasonality in the rainfall regime. Seasonal runoff patterns follow rainfall and rainfall-runoff ratios remain high during the summer—averaging over 50% from November to April and reaching 61% in December despite monthly PET being at near-peak rates. Direct runoff is also high in the summer, accounting for nearly 80% of total catchment discharge. These runoff metrics reflect a highly efficient conversion of precipitation inputs to

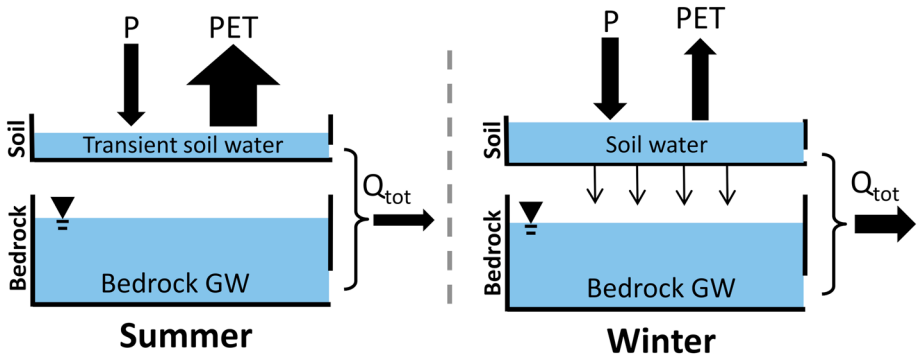

Figure 8. Conceptual model of seasonal catchment water balance fluxes. The width of the black arrows represents the magnitude of the seasonal flux compared to total annual *P*. Summer recharge is absent as a result of higher PET rates and quick storm runoff induced by an efficient soil-based preferential flow path network. Winter recharge occurs as slow diffusive flow through the primary bedrock porosity and is driven by long durations of high catchment wetness conditions. PET = potential evapotranspiration; GW = groundwater.

stream discharge (as noted first by Mosley, 1979, followed by dozens of studies at Maimai thereafter), indicating subsurface stormflow remains a consistent source of runoff generation through all months of year. Yet despite the annually constant rainfall-runoff pattern, our findings show that bedrock recharge exhibits extreme summer-winter seasonality. Paradoxically, the catchment effectively translates precipitation inputs to streamflow across nearly all catchment wetness conditions, yet recharge occurs only under selective catchment conditions, highlighting a complex seasonally shifting internal redistribution process linked to geology and seasonality in ET and antecedent wetness conditions.

5.1. Geological Control on Groundwater Recharge

Groundwater recharge in headwater catchments has been linked directly to the production of event-based subsurface stormflow occurring over fractured bedrock hillslopes (Apples et al., 2015; Hopp & Mcdonnell, 2009). Sprinkler and tracer experiments on steep hillslopes have highlighted fractures as a major conduit to transport water both downslope to supplement storm runoff (Montgomery et al., 1997) and to-depth to recharge deeper aquifer systems (Graham, Van Verseveld, et al., 2010; Tromp-Van Meerveld et al., 2007). Not unexpectedly, volumetric loss of sprinkler water in these fractured systems has been significant, with common observations from 25% and 40% (Graham, Van Verseveld, et al., 2010; Jackson et al., 2016) to extreme cases of more than 90% loss (Tromp-Van Meerveld, et al., 2007). At these, and other fractured sites (Cai & Ofterdinger, 2016; Gleeson et al., 2009; Sukhija et al., 2003), subsurface stormflow or snowmelt water are able to move to depth through fracture pathways over relatively short time scales, allowing direct recharge during individual storm events. Recharge timing and magnitude are thus controlled by the conditions required to initiate subsurface stormflow, the degree of bedrock fracturing and the alignment of fractures with the spatial patterns of stormflow at the soil-bedrock interface.

In contrast, we found that only 0.04% of applied sprinkler water was lost to bedrock during the 96-hr sprinkler experiment at Maimai, an amount equal to just 20 mm of the 4,950 mm of applied rainfall (Figure 3). Our slug tests and the sprinkler experiment revealed low permeability hillslope bedrock that is void of major fracture pathways indicating a distinct lack of secondary porosity within the bedrock structure. Unlike other studied hillslopes, recharge through the bedrock at Maimai occurred through the primary porosity only and over time scales much longer than individual storm events. Although abundant excess moisture exists at the soil-bedrock interface, both as persistent saturation during wet winter months (Figure 8) and as frequent subsurface stormflow during all seasons, recharge is limited by the ability of the geologic formation to slowly move water to depth and not by the availably of water to recharge. As a result, single storm events that generate subsurface stormflow do not drive appreciable recharge despite their considerable frequency (Figure 6e).

5.2. Subsurface Stormflow in Summer but No Summer Recharge?

At Maimai, rainfall occurs on average every 2 days. The 2,600 mm of annual rainfall is distributed nearly evenly between winter (55%) and summer (45%). The frequency of storm events greater than 20 mm—the

approximate storm magnitude needed to initiate subsurface stormflow—is also similar for winter and summer seasons. Our initial hypothesis was that hillslope-scale groundwater recharge would be controlled mostly by event inputs that generate subsurface stormflow and should have minimal seasonality due to the unusually low seasonality in the occurrence, magnitude, and duration of subsurface stormflow events. We rejected this hypothesis since noble gas tracer measurements revealed recharge temperatures nearly 4 °C lower than the local mean annual air temperature (Figure 4). This indicated seasonally specific recharge during colder winter months. This observation was further supported by the distinctly depleted stable isotope composition of bedrock groundwater compared to other catchment waters (e.g., soil water and streamflow). We found that 89% of modeled annual bedrock recharge occurred during the winter months from May to October and 60% of annual modeled recharge resulted from only 25% of annual rainfall during the peak recharge months of June, July, and August. In contrast, during the peak summer months of December, January, and February, nearly the same amount of precipitation produced only 2.4% of annual recharge (Figure 5). This resulted in a recharge efficiency (calculated as depth of recharge divided by depth of rainfall) that was nearly 24-fold higher in peak winter months compared to peak summer months.

Although seasonality of recharge is a widely observed phenomena for larger aquifers and higher order catchments (Jasechko et al., 2014), it has been most often associated with strong intra-annual patterns in precipitation (Descloitres et al., 2008) or in regions where late autumn rainfall and early spring snow melt occur concurrently with low ET demands (Abbott et al., 2000; Jasechko et al., 2017; O'driscoll et al., 2005). Maimai, however, has neither strong intra-annual patterns of precipitation nor a precipitation-ET relationship that is asynchronous. This would point to rainfall magnitude and intensity instead as the primary driver of groundwater recharge, as observed in other rainfall driven recharge systems (Mileham et al., 2009; Owor et al., 2009). However, we found no correlation between recharge and monthly precipitation, wet season precipitation, or annual precipitation totals. Nor did we find a correlation between recharge and the frequency of larger rainfall events (i.e., $>$20 mm) or the magnitude of monthly storm runoff (Q_{dir}). Furthermore, although we did find a correlation between recharge and effective monthly precipitation (P-PET, $R^2 = 0.50$), the strongest relationship existed between recharge and seasonal shifts in PET ($R^2 = 0.72$). Although perhaps not surprising in its own right, taken in context, this recharge seasonality was unexpected at Maimai. Indeed, high summer evaporative budgets have been widely shown to shift recharge timing toward colder seasons (Jasechko et al., 2014, 2017; Scanlon et al., 2006); however, at Maimai despite high summer PET, there still remains high summer runoff.

5.3. Our Groundwater Recharge Model

So how can there be so much summer runoff but no summer recharge? Rainfall-runoff processes at Maimai directly reflect the minimal soil storage capacity (Stewart & Mcdonnell, 1991), low bedrock permeability (Gabrielli et al., 2012), and large quantities of annual rainfall (Pearce et al., 1977). As a result, the catchment is dominated by a highly efficient and extensive preferential flow system capable of delivering large quantities of subsurface stormflow to the stream channel over short periods of time, regardless of the season or antecedent conditions (Graham, Woods, & Mcdonnell, 2010; Mcdonnell, 1990; Mosley, 1982; Weiler et al., 2003).

Figure 8 shows our conceptual model of seasonal recharge and the water balance components at Maimai. During winter, although abundant excess moisture is present within the catchment, low permeability bedrock limits infiltration rates, a process also observed in other humid regions (Sanford, 2002). Saturation at the soil-bedrock interface is frequent, but infiltration rates of the low permeability bedrock are quickly exceeded, creating a form of subsurface infiltration-excess flow at the soil-bedrock interface (as reported in many early studies at the site by Mosley, 1979). Further additions of moisture are either driven laterally downslope to the stream channel or fulfill unrequited soil storage (Mcdonnell, 1990). It is precisely because bedrock infiltration rates are so readily exceeded by the large quantities of rainfall that there is no correlation between rainfall and recharge, either monthly, seasonally, or annually. Thus, in the winter the magnitude of recharge is limited not by the availability of water but by the ability of the geologic formation to transfer water to depth.

During summer, we hypothesize that rainfall events activate the preferential flow network (as they also do in winter) on storm event time scales, thus removing most of the precipitation input from the catchment and limiting the degree to which soil matrix storage is replenished, contrary to the apparent capacity of available soil water storage (Figure 8). Stewart and Mcdonnell (1991) noted specifically that rainfall bypasses the soil

matrix through preferential flow paths and that recharge of the soil matrix occurs more slowly through diffusive processes, thus explaining the high summer stormflow yet no summer recharge and the lack of correlation between recharge and either total precipitation or frequency of subsurface stormflow. The increase in soil water storage that does occur during summer events is quickly depleted between events by the much greater summer ET flux, and soil water that would otherwise slowly percolate deeper as bedrock recharge is lost instead to evaporative processes. Under this scenario, the catchment experiences episodic high wetness conditions that produce large volumes of runoff. But, critically, the long periods of extended wetness needed for recharge that occur in the winter are not attained, and bedrock recharge rates fall to near 0 during the warmer summer season.

The lack of correlation between recharge magnitude and precipitation or runoff metrics is noteworthy as most large-scale recharge models used to inform groundwater sustainability have shown trends in recharge that widely track future changes in precipitation (both positively and negatively, due to competing feedbacks; Taylor, Scanlon, et al., 2013). We show here, however, that geologic structure and seasonal trends in evaporation that determine the duration of very wet conditions at the soil-bedrock interface instead are the primary control on recharge. Thus, future changes in annual precipitation at Maimai will likely have little effect on changes in groundwater recharge.

6. Conclusion

The hydrologic system at the Maimai watershed—where little apparent seasonality exists in precipitation or catchment runoff metrics—possesses extreme seasonality in bedrock groundwater recharge timing. Our analysis of bedrock groundwater isotopic signatures and noble gas temperatures revealed that groundwater recharge occurs almost exclusively during the cold season. A simple empirical recharge model and extensive bedrock characterization associated with a bedrock surface sprinkler experiment supported the findings of the linkage between the seasonality of bedrock groundwater recharge and the geologic controls imposed by the bedrock structure. Our work suggests that the unfractured and low permeability bedrock directly controls the timing of bedrock recharge. The absence of considerable secondary porosity allows only diffuse recharge to occur—limiting recharge timing to conditions of extended periods of high catchment wetness. We found that summer-winter climate seasonality and geologic characteristics, as opposed to the frequency of subsurface stormflow production, imparts the critical control on the timing of recharge. During winter, under high catchment wetness conditions, the bedrock permeability is the rate limiting control on recharge amounts. While in the summer, high evaporation rates combined with efficient hillslope drainage through preferential flow paths eliminates excess moisture in the catchment that would otherwise percolate toward the water table. Critically, the lack of secondary porosity in the bedrock prevents subsurface stormflow from moving to depth quickly, resulting in the observed high summer runoff ratios with minimal groundwater recharge.

With recent work highlighting the importance of headwaters as focal recharge zones for downslope aquifers (Jasechko et al., 2016), our work helps to understand how hydroclimatic and geologic variables combine to control groundwater recharge. While future projections of groundwater recharge under various climate change scenarios are largely associated with changes in precipitation (Taylor, Scanlon, et al., 2013) and that precipitation intensity and magnitude control recharge timing and rates (Allen et al., 2010; Owor et al., 2009; Taylor, Todd, et al., 2013), our work is a cautionary tale. For such studies using precipitation or runoff to directly estimate recharge, Maimai is a clear example of a headwater aquifer that shows no relationship to precipitation amount or timing, despite catchment runoff dynamics that indicate a clear abundance of excess moisture in the system year-round.

Acknowledgments
This work was supported through funding by NSERC Discovery grant to Jeffrey McDonnell and the Horton Hydrology Research Grant from the American Geophysical Union to Chris Gabrielli. We thank Uwe Morgenstern for the noble gas analysis and for useful discussions along the way. We also thank Mike Stewart, Garth Vanderkamp, Lee Barbour, and Andrew Ireson for useful comments on various aspects of this work along the way. We thank John Payne at Landcare Research and Matt Taylor and Christie Thomson for their invaluable assistance and support in the field and throughout the extended field campaign in New Zealand. We thank the three reviewers for the help with significantly improving the presentation of the final manuscript. No real or perceived financial conflicts of interests exist for any author. Data supporting the conclusions can be obtained within references and tables where appropriate, and through this DOI: 10.17605/OSF.IO/JU6A3.

References

Abbott, M., Lini, A., & Bierman, P. (2000). $\delta^{18}O$, δD and ^{3}H measurements constrain groundwater recharge patterns in an upland fractured bedrock aquifer, Vermont, USA. *Journal of Hydrology*, *228*(1), 101–112. https://doi.org/10.1016/S0022-1694(00)00149-9

Ali, G. A., L'heureux, C., Roy, A. G., Turmel, M.-C., & Courchesne, F. (2011). Linking spatial patterns of perched groundwater storage and stormflow generation processes in a headwater forested catchment. *Hydrological Processes*, *25*(25), 3843–3857. https://doi.org/10.1002/hyp.8238

Allen, D., Whitfield, P., & Werner, A. (2010). Groundwater level responses in temperate mountainous terrain: Regime classification, and linkages to climate and streamflow. *Hydrological Processes*, *24*(23), 3392–3412. https://doi.org/10.1002/hyp.7757

Ameli, A., Craig, J., & Mcdonnell, J. (2015). Are all runoff processes the same? Numerical experiments comparing a Darcy-Richards solver to an overland flow-based approach for subsurface storm runoff simulation. *Water Resources Research*, *51*, 10008–10028. https://doi.org/10.1002/2015WR017199

Anderson, M. G., & Mcdonnell, J. J. (2005). *Encyclopedia of hydrological sciences*. Hoboken, N.J: John Wiley & Sons. https://doi.org/10.1002/0470848944

Appels, W. M., Graham, C. B., Freer, J. E., & Mcdonnell, J. J. (2015). Factors affecting the spatial pattern of bedrock groundwater recharge at the hillslope scale. *Hydrological Processes*, *29*(21), 4594–4610. https://doi.org/10.1002/hyp.10481

Asano, Y., Uchida, T., & Ohte, N. (2002). Residence times and flow paths of water in steep unchannelled catchments, Tanakami, Japan. *Journal of Hydrology*, *261*(1-4), 173–192. https://doi.org/10.1016/S0022-1694(02)00005-7

Bachmair, S., Weiler, M., & Troch, P. A. (2012). Intercomparing hillslope hydrological dynamics: Spatio-temporal variability and vegetation cover effects. *Water Resources Research*, *48*, W05537. https://doi.org/10.1029/2011WR011196

Berghuijs, W. R., Sivapalan, M., Woods, R. A., & Savenije, H. H. G. (2014). Patterns of similarity of seasonal water balances: A window into streamflow variability over a range of time scales. *Water Resources Research*, *50*, 5638–5661. https://doi.org/10.1002/2014WR015692

Blöschl, G., Hall, J., Parajka, J., Perdigão, R. A., Merz, B., Arheimer, B., et al. (2017). Changing climate shifts timing of European floods. *Science*, *357*(6351), 588–590. https://doi.org/10.1126/science.aan2506

Bohlke, J. & Krantz, D.E. (2003). Isotope geochemistry and chronology of offshore ground water beneath Indian River Bay, Delaware, US Department of the Interior, US Geological Survey.

Bowen, F. (1967). Early Pleistocene glacial and associated deposits of the West Coast of the South Island, New Zealand. *New Zealand Journal of Geology and Geophysics*, *10*(1), 164–181. https://doi.org/10.1080/00288306.1967.10428188

Brooks, E. S., Boll, J., & Mcdaniel, P. A. (2004). A hillslope-scale experiment to measure lateral saturated hydraulic conductivity. *Water Resources Research*, *40*, W04208. https://doi.org/10.1029/2003WR002858

Buttle, J. M., & Mcdonald, D. J. (2002). Coupled vertical and lateral preferential flow on a forested slope. *Water Resources Research*, *38*(5), 1060. https://doi.org/10.1029/2001WR000773

Cai, Z., & Ofterdinger, U. (2016). Analysis of groundwater-level response to rainfall and estimation of annual recharge in fractured hard rock aquifers, NW Ireland. *Journal of Hydrology*, *535*, 71–84. https://doi.org/10.1016/j.jhydrol.2016.01.066

Descloitres, M., Ruiz, L., Sekhar, M., Legchenko, A., Braun, J. J., Kumar, M., & Subramanian, S. (2008). Characterization of seasonal local recharge using electrical resistivity tomography and magnetic resonance sounding. *Hydrological Processes*, *22*(3), 384–394. https://doi.org/10.1002/hyp.6608

Ebel, B. A., & Loague, K. (2006). Physics-based hydrologic-response simulation: Seeing through the fog of equifinality. *Hydrological Processes*, *20*(13), 2887–2900. https://doi.org/10.1002/hyp.6388

Gabrielli, C. P., Mcdonnell, J. J., & Jarvis, W. T. (2012). The role of bedrock groundwater in rainfall–runoff response at hillslope and catchment scales. *Journal of Hydrology*, *450*, 117–133. https://doi.org/10.1016/j.jhydrol.2012.05.023

Gabrielli, C. P., Morgenstern, U., Stewart, M., & Mcdonnell, J. J. (2018). Contrasting groundwater and streamflow ages at the Maimai watershed. *Water Resources Research* https://doi.org/10.1029/2017WR021825, *54*, 3937–3957. https://doi.org/10.1029/2017WR021825

Gleeson, T., Novakowski, K., & Kurt Kyser, T. (2009). Extremely rapid and localized recharge to a fractured rock aquifer. *Journal of Hydrology*, *376*(3–4), 496–509. https://doi.org/10.1016/j.jhydrol.2009.07.056

Graham, C. B., Van Verseveld, W., Barnard, H. R., & Mcdonnell, J. J. (2010). Estimating the deep seepage component of the hillslope and catchment water balance within a measurement uncertainty framework. *Hydrological Processes*, *24*(25), 3631–3647. https://doi.org/10.1002/hyp.7788

Graham, C. B., Woods, R. A., & Mcdonnell, J. J. (2010). Hillslope threshold response to rainfall: (1) A field based forensic approach. *Journal of Hydrology*, *393*(1-2), 65–76. https://doi.org/10.1016/j.jhydrol.2009.12.015

Grant, G. E., & Dietrich, W. E. (2017). The frontier beneath our feet. *Water Resources Research*, *53*, 2605–2609. https://doi.org/10.1002/2017WR020835

Harr, R. D. (1977). Water flux in soil and subsoil on a steep forested slope. *Journal of Hydrology*, *33*, 37–58. https://doi.org/10.1016/0022-1694(77)90097-X

Heaton, T. H. E., & Vogel, J. C. (1981). "Excess air" in groundwater. *Journal of Hydrology*, *50*, 201–216. https://doi.org/10.1016/0022-1694(81)90070-6

Heppner, C. S., Nimmo, J. R., Folmar, G. J., Gburek, W. J., & Risser, D. W. (2007). Multiple-methods investigation of recharge at a humid-region fractured rock site, Pennsylvania, USA. *Hydrogeology Journal*, *15*(5), 915–927. https://doi.org/10.1007/s10040-006-0149-6

Hewlett, J. D., & Hibbert, A. R. (1967). In W. E. Sopper, & H. W. Lull (Eds.), *Forest hydrology*, (pp. 275–291). New York: Pergamon Press.

Hopp, L., & Mcdonnell, J. J. (2009). Connectivity at the hillslope scale: Identifying interactions between storm size, bedrock permeability, slope angle and soil depth. *Journal of Hydrology*, *376*(3–4), 378–391. https://doi.org/10.1016/j.jhydrol.2009.07.047

Hvorslev, M.J. (1951). Time lag and soil permeability in ground-water observations. *No. WES-BULL-36*, Army Engineer Waterways Experiment Station Vicksburg MS.

Jackson, C. R., Du, E., Klaus, J., Griffiths, N. A., Bitew, M., & Mcdonnell, J. J. (2016). Interactions among hydraulic conductivity distributions, subsurface topography, and transport thresholds revealed by a multitracer hillslope irrigation experiment. *Water Resources Research*, *52*, 6186–6206. https://doi.org/10.1002/2015WR018364

Jasechko, S., Birks, S. J., Gleeson, T., Wada, Y., Fawcett, P. J., Sharp, Z. D., et al. (2014). The pronounced seasonality of global groundwater recharge. *Water Resources Research*, *50*, 8845–8867. https://doi.org/10.1002/2014WR015809

Jasechko, S., Kirchner, J. W., Welker, J. M., & Mcdonnell, J. J. (2016). Substantial proportion of global streamflow less than three months old. *Nature Geoscience*, *9*(2), 126–129. https://doi.org/10.1038/ngeo2636

Jasechko, S., Wassenaar, L. I., & Mayer, B. (2017). Isotopic evidence for widespread cold-season-biased groundwater recharge and young streamflow across central Canada. *Hydrological Processes*, *31*(6), 2196–2209. https://doi.org/10.1002/hyp.11175

Jencso, K. G., & Mcglynn, B. L. (2011). Hierarchical controls on runoff generation: Topographically driven hydrologic connectivity, geology, and vegetation. *Water Resources Research*, *47*, W11527. https://doi.org/10.1029/2011WR010666

Kendall, C., & Mcdonnell, J. J. (1998). *Isotope tracers in catchment hydrology*. Amsterdam: Elsevier.

Kendy, E., Gérard-Marchant, P., Todd Walter, M., Zhang, Y., Liu, C., & Steenhuis, T. S. (2003). A soil-water-balance approach to quantify groundwater recharge from irrigated cropland in the North China Plain. *Hydrological Processes*, *17*(10), 2011–2031. https://doi.org/10.1002/hyp.1240

Kosugi, K. I., Katsura, S. Y., Katsuyama, M., & Mizuyama, T. (2006). Water flow processes in weathered granitic bedrock and their effects on runoff generation in a small headwater catchment. *Water Resources Research*, *42*, W02414. https://doi.org/10.1029/2005WR004275

Lim, K. J., Engel, B. A., Tang, Z., Choi, J., Kim, K. S., Muthukrishnan, S., & Tripathy, D. (2005). Automated web GIS based hydrograph analysis tool, WHAT. *JAWRA Journal of the American Water Resources Association*, *41*(6), 1407–1416. https://doi.org/10.1111/j.1752-1688.2005.tb03808.x

Lindsay, W. L. (1979). *Chemical equilibria in soils*. Chichester, Sussex: John Wiley and Sons Ltd.
Mcdonnell, J. J. (1990). A rationale for old water discharge through macropores in a steep, humid catchment. *Water Resources Research*, *26*(11), 2821–2832. https://doi.org/10.1029/WR026i011p02821
Mcdonnell, J. J. (2013). Are all runoff processes the same? *Hydrological Processes*, *27*(26), 4103–4111. https://doi.org/10.1002/hyp.10076
Mcglynn, B. L., Mcdonnel, J. J., & Brammer, D. D. (2002). A review of the evolving perceptual model of hillslope flowpaths at the Maimai catchments, New Zealand. *Journal of Hydrology*, *257*(1-4), 1–26. https://doi.org/10.1016/S0022-1694(01)00559-5
Mcglynn, B. L., Mcdonnell, J. J., Seibert, J., & Kendall, C. (2004). Scale effects on headwater catchment runoff timing, flow sources, and groundwater-streamflow relations. *Water Resources Research*, *40*, W07504. https://doi.org/10.1029/2003WR002494
Mileham, L., Taylor, R. G., Todd, M., Tindimugaya, C., & Thompson, J. (2009). The impact of climate change on groundwater recharge and runoff in a humid, equatorial catchment: Sensitivity of projections to rainfall intensity. *Hydrological Sciences Journal*, *54*(4), 727–738. https://doi.org/10.1623/hysj.54.4.727
Milly, P. C. D. (1994). Climate, soil water storage, and the average annual water balance. *Water Resources Research*, *30*(7), 2143–2156. https://doi.org/10.1029/94WR00586
Montgomery, D. R., Dietrich, W. E., Torres, R., Anderson, S. P., Heffner, J. T., & Loague, K. (1997). Hydrologic response of a steep, unchanneled valley to natural and applied rainfall. *Water Resources Research*, *33*(1), 91–109. https://doi.org/10.1029/96WR02985
Mortimer, N., Sutherland, R., & Nathan, S. (2001). Torlesse greywacke and Haast Schist source for Pliocene conglomerates near Reefton, New Zealand. *New Zealand Journal of Geology and Geophysics*, *44*(1), 105–111. https://doi.org/10.1080/00288306.2001.9514927
Mosley, M. P. (1979). Streamflow generation in a forested watershed. *Water Resources Research*, *15*, 795–806. https://doi.org/10.1029/WR015i004p00795
Mosley, M. P. (1982). Subsurface flow velocities through selected forest soils, South Island, New Zealand. *Journal of Hydrology*, *55*, 65–92. https://doi.org/10.1016/0022-1694(82)90121-4
Niu, Y., Castro, M. C., Hall, C. M., Gingerich, S. B., Scholl, M. A., & Warrier, R. B. (2017). Noble gas signatures in the Island of Maui, Hawaii: Characterizing groundwater sources in fractured systems. *Water Resources Research*, *53*, 3599–3614. https://doi.org/10.1002/2016WR020172
O'driscoll, M. A., Dewalle, D. R., Mcguire, K. J., & Gburek, W. J. (2005). Seasonal ^{18}O variations and groundwater recharge for three landscape types in central Pennsylvania, USA. *Journal of Hydrology*, *303*(1-4), 108–124. https://doi.org/10.1016/j.jhydrol.2004.08.020
Owor, M., Taylor, R., Tindimugaya, C., & Mwesigwa, D. (2009). Rainfall intensity and groundwater recharge: Empirical evidence from the Upper Nile Basin. *Environmental Research Letters*, *4*(3), 035009. https://doi.org/10.1088/1748-9326/4/3/035009
Pearce, A.J., O'loughlin, C.L. & Rowe, L.K. (1977). Hydrologic regime of small, undisturbed beech forest catchments, North Westland. *Inf Ser NZ Dep Sci Ind Res*.
Peters, D. L., Buttle, J. M., Taylor, C. H., & Lazerte, B. D. (1995). Runoff production in a forested, shallow soil, Canadian Shield basin. *Water Resources Research*, *31*(5), 1291–1304. https://doi.org/10.1029/94WR03286
Petersen, T., Devineni, N., & Sankarasubramanian, A. (2012). Seasonality of monthly runoff over the continental United States: Causality and relations to mean annual and mean monthly distributions of moisture and energy. *Journal of Hydrology*, *468-469*, 139–150. https://doi.org/10.1016/j.jhydrol.2012.08.028
Sanford, W. (2002). Recharge and groundwater models: an overview. *Hydrogeology Journal*, *10*(1), 110–120. https://doi.org/10.1007/s10040-001-0173-5
Scanlon, B. R., Keese, K. E., Flint, A. L., Flint, L. E., Gaye, C. B., Edmunds, W. M., & Simmers, I. (2006). Global synthesis of groundwater recharge in semiarid and arid regions. *Hydrological Processes*, *20*(15), 3335–3370. https://doi.org/10.1002/hyp.6335
Sklash, M. G., & Farvolden, R. N. (1979). The role of groundwater in storm runoff. *Journal of Hydrology*, *43*, 45–65. https://doi.org/10.1016/0022-1694(79)90164-1
Stewart, M. K., & Mcdonnell, J. J. (1991). Modeling base flow soil water residence times from deuterium concentrations. *Water Resources Research*, *27*(10), 2681–2693. https://doi.org/10.1029/91WR01569
Sukhija, B., Reddy, D., Nagabhushanam, P., & Hussain, S. (2003). Recharge processes: piston flow vs preferential flow in semi-arid aquifers of India. *Hydrogeology Journal*, *11*(3), 387–395. https://doi.org/10.1007/s10040-002-0243-3
Tang, Y., & Wang, D. (2017). Evaluating the role of watershed properties in long-term water balance through a Budyko equation based on two-stage partitioning of precipitation. *Water Resources Research*, *53*, 4142–4157. https://doi.org/10.1002/2016WR019920
Taylor, R. G., Scanlon, B., Döll, P., Rodell, M., Van Beek, R., Wada, Y., et al. (2013). Ground water and climate change. *Nature Climate Change*, *3*(4), 322–329. https://doi.org/10.1038/nclimate1744
Taylor, R. G., Todd, M. C., Kongola, L., Maurice, L., Nahozya, E., Sanga, H., & Macdonald, A. M. (2013). Evidence of the dependence of groundwater resources on extreme rainfall in East Africa. *Nature Climate Change*, *3*(4), 374–378. https://doi.org/10.1038/nclimate1731
Tetzlaff, D., Birkel, C., Dick, J., Geris, J., & Soulsby, C. (2014). Storage dynamics in hydropedological units control hillslope connectivity, runoff generation, and the evolution of catchment transit time distributions. *Water Resources Research*, *50*, 969–985. https://doi.org/10.1002/2013WR014147
Thornthwaite, C. W. (1948). An approach toward a rational classification of climate. *Geographical Review*, *38*(1), 55–94. https://doi.org/10.2307/210739
Tromp-Van Meerveld, H., & Mcdonnell, J. (2006). Threshold relations in subsurface stormflow: 1. A 147-storm analysis of the Panola hillslope. *Water Resources Research*, *42*, W02410. https://doi.org/10.1029/2004WR003778
Tromp-Van Meerveld, H., Peters, N., & Mcdonnell, J. (2007). Effect of bedrock permeability on subsurface stormflow and the water balance of a trenched hillslope at the Panola Mountain Research Watershed, Georgia, USA. *Hydrological Processes*, *21*(6), 750–769. https://doi.org/10.1002/hyp.6265
Van Verseveld, W. J., Barnard, H. R., Graham, C. B., Mcdonnell, J. J., Brooks, J. R., & Weiler, M. (2017). A sprinkling experiment to quantify celerity-velocity differences at the hillslope scale. *Hydrology and Earth System Sciences Discussions*, 1–39. https://doi.org/10.5194/hess-2017-125
Weiler, M., Mcglynn, B. L., Mcguire, K. J., & Mcdonnell, J. J. (2003). How does rainfall become runoff? A combined tracer and runoff transfer function approach. *Water Resources Research*, *39*(11), 1315. https://doi.org/10.1029/2003WR002331
Wienhöfer, J., & Zehe, E. (2014). Predicting subsurface stormflow response of a forested hillslope–the role of connected flow paths. *Hydrology and Earth System Sciences*, *18*(1), 121–138. https://doi.org/10.5194/hess-18-121-2014
Woods, R., & Rowe, L. (1996). The changing spatial variability of subsurface flow across a hillside. *Journal of Hydrology. New Zealand*, *35*(1), 51–86.
Wu, J., Zhang, R., & Yang, J. (1996). Analysis of rainfall-recharge relationships. *Journal of Hydrology*, *177*(1), 143–160. https://doi.org/10.1016/0022-1694(95)02935-4
Xu, C. Y., & Chen, D. (2005). Comparison of seven models for estimation of evapotranspiration and groundwater recharge using lysimeter measurement data in Germany. *Hydrological Processes*, *19*(18), 3717–3734. https://doi.org/10.1002/hyp.5853